STABLE LIMIT CYCLES AS TUNABLE SIGNAL SOURCES

Wolfram E. Weingartner

Unaffiliated Researcher
Enns, Austria
ww@701.media

ABSTRACT

This paper presents a method for synthesizing audio signals from nonlinear dynamical systems exhibiting stable limit cycles, with control over frequency and amplitude independent of changes to the system's internal parameters. Using the van der Pol oscillator and the Brusselator as case studies, it is demonstrated how parameters are decoupled from frequency and amplitude by rescaling the angular frequency and normalizing amplitude extrema. Practical implementation considerations are discussed, as are the limits and challenges of this approach. The method's validity is evaluated experimentally and synthesis examples show the application of tunable nonlinear oscillators in sound design, including the generation of transients in FM synthesis by means of a van der Pol oscillator and a Supersaw oscillator bank based on the Brusselator.

1. INTRODUCTION

Nonlinear dynamical systems are systems whose evolution over time is governed by nonlinear differential equations. Unlike linear systems, nonlinear systems can exhibit periodic, quasiperiodic, and chaotic behaviors, making them attractive for the synthesis of complex waveforms. There is a vast amount of literature surrounding the use of nonlinear systems in sound synthesis (e.g. [1, 2, 3]), often with a particular focus on modeling nonlinear phenomena in musical instruments (e.g. [4, 5, 6]).

Stable limit cycles are one class of periodic solutions that can arise in such systems. Due to their inherent periodicity, limit cycles lend themselves as sources for pitched sound signals. Their appeal lies in their often rich harmonic content, the availability of parameters that alter timbre in complex ways, and the possibility of extending them to quasiperiodic or chaotic regimes using nonautonomous modifications. However, it appears that much of the existing literature treats them as incidental to the system's behavior rather than as a primary signal source for sound synthesis. Furthermore, little attention has been given to the challenge of making such systems tunable: in many nonlinear systems, parameters simultaneously influence the period, amplitude, offset, and harmonic structure of the limit cycle. As a result, frequency cannot be adjusted independently without distorting other aspects of the signal in undesirable ways.

This paper presents a conceptually simple method that enables the synthesis of antialiased and amplitude-normalized signals from limit cycles with arbitrarily chosen frequency and amplitude, both of which remain approximately stable even when the system's parameters vary over time. "Approximately" here refers to limitations introduced by numerical integration, convergence time, and approximations of certain properties of the limit cycle. The method is motivated in part by previous projects [7, 8, 9] that use limit cycles in sound synthesis, but lack tuning stability.

Section 2 describes systems that are well-suited to audio signal generation based on limit cycles and explores connections between their mathematical form and their resulting waveforms. Section 3 presents the proposed approach for synthesizing tunable, normalized, amplitude-stable signals from limit cycles, along with discussion of its prerequisites, limitations, and implementation considerations. Section 4 evaluates the proposed method and showcases experimental applications of the method in audio synthesis. Finally, Section 5 summarizes the main findings and outlines potential directions for future work.

2. SYSTEMS EXHIBITING LIMIT CYCLES

This section focuses on autonomous systems of the form

$$\begin{aligned} \frac{\mathrm{d}x}{\mathrm{d}t} &= \Phi_1(x, y), \\ \frac{\mathrm{d}y}{\mathrm{d}t} &= \Phi_2(x, y), \end{aligned} \tag{1}$$

where $x(t)$ and $y(t)$ describe the system's state at time t, and Φ_1 and Φ_2 are nonlinear functions defining the system's dynamics. The state of the system at time t corresponds to a point $(x(t), y(t))$ in phase space. Its evolution over time traces out a trajectory determined by the vector field defined by (1) and starting with initial condition $(x(0), y(0))$.

A closed orbit is a trajectory that repeats itself at some period T, such that $(x(t+T), y(t+T)) = (x(t), y(t))$ for all t. Such a closed orbit is called a stable limit cycle if it is isolated. In other words, it attracts nearby trajectories and is therefore the only closed orbit in its neighborhood.

In general, proving the existence of stable limit cycles is a nontrivial task [10]. This paper focuses on systems in which a stable limit cycle is proven to be globally unique by well-known theorems or sufficiently isolated, meaning that no other nearby attractors can be reached through small perturbations. While nonlinear systems can have multiple coexisting stable limit cycles (multistability), such cases are avoided here to sidestep the additional complexity associated with handling multiple regions of attraction. Although multistable systems may offer interesting behavior for audio synthesis, as will be mentioned in Section 5, they are beyond the scope of this work.

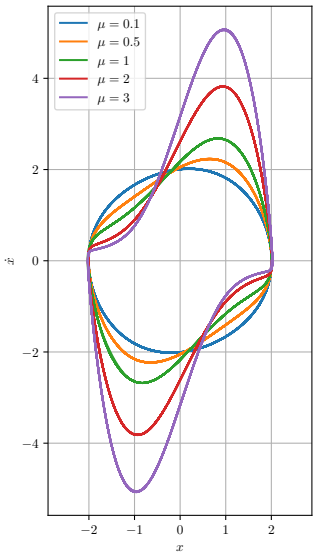

Figure 1: Limit cycles of the van der Pol oscillator for various μ.

2.1. Liénard Systems

Liénard systems are of the form

$$\begin{aligned} \frac{\mathrm{d}x}{\mathrm{d}t} &= y, \\ \frac{\mathrm{d}y}{\mathrm{d}t} &= -g(x) - f(x)y, \end{aligned} \tag{2}$$

or, equivalently, in one-dimensional second-order form,

$$\frac{\mathrm{d}^2x}{\mathrm{d}t^2} + f(x)\frac{\mathrm{d}x}{\mathrm{d}t} + g(x) = 0, \tag{3}$$

where x is the system's displacement at time t, $f(x)$ is a damping function controlling how energy is injected into and dissipated from the system, and $g(x)$ is a restoring-force function controlling the system's tendency to return to equilibrium.

Liénard systems are of particular interest here because their waveforms and the harmonic structure of their limit cycles can be qualitatively inferred to some degree by inspecting the shapes of $f(x)$ and $g(x)$. Additionally, under certain conditions, such systems are guaranteed to exhibit a unique, stable limit cycle according to Liénard's theorem [10]. The original version of Liénard's theorem requires that $f(x)$ be even and $g(x)$ be odd, which ensures that the resulting limit cycle is point-symmetric, as can be visually verified by inspecting Figure 1. If the audio signal is synthesized from the limit cycle by a linear projection, the resulting wave only has odd harmonics. Recent generalizations, such as those by Villari et al. [11] and Hayashi et al. [12], weaken the symmetry requirements on $f(x)$ and $g(x)$, such that point symmetry of the limit cycle is no longer guaranteed.

2.1.1. Case Study: Van der Pol Oscillator

The van der Pol oscillator, introduced in 1920 by Dutch physicist Balthasar van der Pol to model oscillating currents in triode circuits [13], is a classical example of a nonlinear system exhibiting

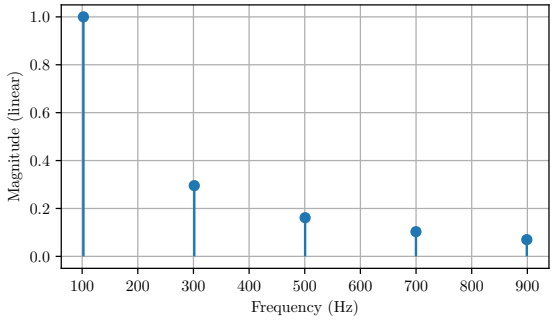

Figure 2: Harmonics of a 100 Hz wave synthesized by the van der Pol oscillator with $\mu = 5$ and projection $(x(t), y(t)) \mapsto x(t)$.

a stable limit cycle. It fits the forms of (2) and (3) with

$$\begin{aligned} f(x) &= -\mu\big(1 - x^2\big), \\ g(x) &= x, \end{aligned} \tag{4}$$

where the parameter $\mu \geq 0$ controls the system's nonlinear damping. For $\mu = 0$, the system reduces to a simple harmonic oscillator, which has infinitely many periodic solutions but no limit cycle. For $\mu > 0$, the damping function causes the system to inject energy if $|x| < 1$ and to dissipate energy if $|x| > 1$, giving rise to a limit cycle where these effects balance [10].

Since $f(x)$ is even and $g(x)$ is odd, we expect the resulting linearly projected waveform to be symmetric and contain only odd harmonics. Figure 1 shows limit cycles for various μ. Figure 2 displays the harmonics of a 100 Hz wave generated by the van der Pol oscillator and confirms that only odd harmonics are present.

By relaxing the symmetries of $f(x)$ or $g(x)$, we can modify (4) to produce even harmonics in addition to odd ones. Importantly, these modifications must still follow the conditions established in [12], which are omitted here for brevity. One of many possible modifications is

$$\begin{aligned} f(x) &= \mu\big(1 + x - x^2\big), \\ g(x) &= e^x - 1. \end{aligned} \tag{5}$$

Figure 3 shows this modified oscillator's harmonics.

2.2. Designed Systems

It is possible to design systems that have a unique, stable limit cycle by construction. This can be useful, for example, when allowing the damping parameter μ of the van der Pol oscillator to be dynamically modulated in a synthesizer application, although this also leads to a subtle but significant issue: As $\mu \to 0$, the system converges to the limit cycle increasingly slowly and for $\mu = 0$, it reduces to a simple harmonic oscillator with magnitude $\|(x(t), y(t))\|$. Depending on x and y, the waveform's amplitude can temporarily or permanently become much too small or much too large.

One way to mitigate this, while approximately preserving the van der Pol oscillator's behavior at low μ, is to design a system with a circular limit cycle and interpolate it with the original oscillator based on the value of μ. The circular limit cycle mimicks

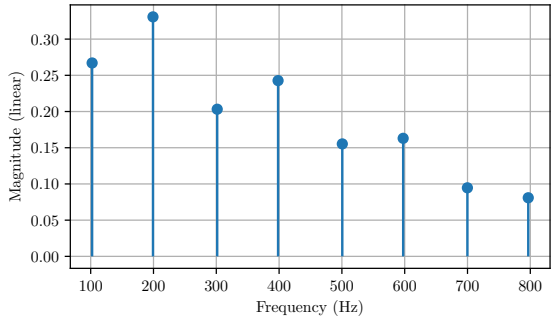

Figure 3: Harmonics of a 100 Hz wave generated by the asymmetrical Liénard system (5) with $\mu = 5$.

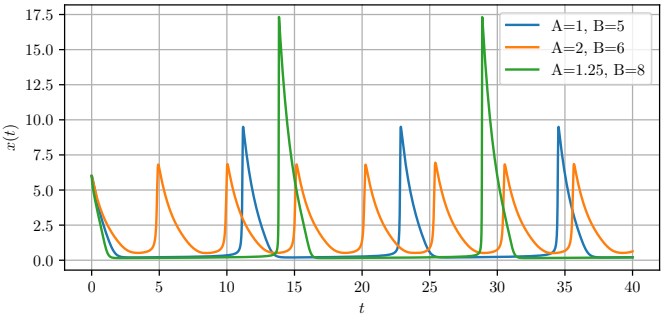

Figure 4: $x(t)$ time series of Brusselator solutions with different parameter choices.

the harmonic oscillator but additionally acts as an attractor. Such a system can be defined in polar coordinates as

$$\begin{aligned} \frac{\mathrm{d}r}{\mathrm{d}t} &= R - r, \\ \frac{\mathrm{d}\theta}{\mathrm{d}t} &= \omega, \end{aligned} \tag{6}$$

where R is the limit cycle's desired radius, and ω is the angular frequency. Transforming (6) to Cartesian coordinates yields

$$\begin{aligned} \frac{\mathrm{d}x_\mathrm{r}}{\mathrm{d}t} &= x_\mathrm{r}\left(\frac{R}{\sqrt{x_\mathrm{r}^2 + y_\mathrm{r}^2}} - 1\right) - \omega y_\mathrm{r}, \\ \frac{\mathrm{d}y_\mathrm{r}}{\mathrm{d}t} &= y_\mathrm{r}\left(\frac{R}{\sqrt{x_\mathrm{r}^2 + y_\mathrm{r}^2}} - 1\right) + \omega x_\mathrm{r}. \end{aligned} \tag{7}$$

Next, we recall the van der Pol equation from (4), rewrite it in the two-dimensional form of (2), and interpolate it with (7) using an interpolation factor τ to obtain

$$\begin{aligned} \frac{\mathrm{d}x}{\mathrm{d}t} &= \tau y - (1-\tau)\frac{\mathrm{d}x_\mathrm{r}}{\mathrm{d}t}, \\ \frac{\mathrm{d}y}{\mathrm{d}t} &= \tau\big(\mu(1-x^2)y - x\big) - (1-\tau)\frac{\mathrm{d}y_\mathrm{r}}{\mathrm{d}t}, \end{aligned} \tag{8}$$

where $\tau = \min(\mu, 1)$. For simplicity, we set $\omega = 1$ and $R = 2$, which is approximately equal to the magnitude of the x component of the van der Pol oscillator's limit cycle for all $\mu > 0$ [14].

This serves as an example of a dynamical system designed to exhibit a unique stable limit cycle with an appropriate shape. More general approaches for constructing systems with arbitrarily shaped limit cycles are described by Pasandi et al. [15].

2.3. Other Systems

Beyond Liénard-type and explicitly designed systems, there are many other systems known to exhibit stable and unique, or sufficiently isolated, limit cycles for certain parameter choices. Examples include the Rayleigh oscillator [16], the Duffing oscillator [17], and the Sel'kov glycolysis model [18].

2.3.1. Case Study: Brusselator

Another example is the Brusselator, a theoretical model of autocatalytic chemical reactions propsed by Prigogine and Lefever [19] in 1968 in Brussels. The system is governed by

$$\begin{aligned} \frac{\mathrm{d}x}{\mathrm{d}t} &= A - (B+1)x + x^2 y, \\ \frac{\mathrm{d}y}{\mathrm{d}t} &= x(B - xy), \end{aligned} \tag{9}$$

where A and B are unitless parameters, originally representing concentrations of two reactants.

The Brusselator exhibits a stable limit cycle if $B > 1 + A^2$ [20]. Unlike the van der Pol oscillator, it is not centered at the origin of the phase plane. In fact, its location is a function of both A and B. Furthermore, while the x component of the van der Pol oscillator's limit cycle has magnitude near 2 for all μ [14], the shape and size of the Brusselator's limit cycle varies significantly for different A and B.

As can be seen in Figure 4, the Brusselator can be used to synthesize waveforms resembling sawtooth waves to some degree.

3. SIGNAL SYNTHESIS

One factor limiting the practical use of limit cycle-based synthesis is that parameter changes typically alter the period and amplitude of the resulting signals in musically often inconvenient ways. In this section, we derive a conceptually simple method for synthesizing audio signals from limit cycles at a desired frequency and amplitude which remain approximately stable under parameter modulation. Further, the method's limitations and some implementation concerns are discussed.

3.1. Derivation

We begin by observing that the phase portrait of a simple harmonic oscillator is a circle whose radius corresponds to the desired signal magnitude. For the purpose of this derivation, we treat limit cycles as distorted and possibly translated deformations of this circular trajectory. To simplify the analysis, we ignore convergence behavior and assume that the system's state is on the limit cycle and remains there at all times.

3.1.1. Period Compensation

For a sinusoid with unity amplitude and angular frequency ω, we have

$$x(t) = \sin(\omega t), \tag{10}$$

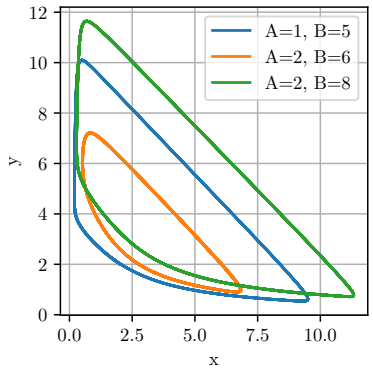

Figure 5: Limit cycles of the Brusselator for different parameters.

where the angular frequency is traditionally defined as

$$\omega = \frac{2\pi}{T}. \tag{11}$$

Recognizing that the angular frequency is a ratio of the trajectory's angular period and the period T corresponding to the desired frequency f, we can define a generalized angular frequency

$$\hat{\omega} = \frac{T_{\text{ang}}(\mathbf{p})}{T}, \tag{12}$$

where T_{ang} is the trajectory's angular period as a function of parameter vector $\mathbf{p}$. This vector consists of all system parameters that affect the trajectory's geometry. For example, for the van der Pol oscillator, $\mathbf{p}_{\text{VDP}} = (\mu)$, and for the Brusselator $\mathbf{p}_{\text{Brussel}} = (A, B)$.

Since nonlinear systems are not generally solvable in closed form, we cannot expect a symbolic expression for T_{ang}. Instead, we will later discuss in Section 3.2.1 how to obtain approximations for T_{ang} numerically by estimating it from the system's behavior.

3.1.2. Amplitude Normalization

Unlike the simple harmonic oscillator, whose amplitude we assume to be normalized to ± 1, the amplitude of a limit cycle can vary significantly as system parameters change. For instance, as illustrated in Figure 5, the Brusselator's limit cycle not only shifts in location, thereby introducing a DC offset, but also changes in size, which can result in clipping and unwanted amplitude fluctuations when parameters are modulated.

Assuming we know certain properties about the limit cycle, normalization terms are easily devised. The quantities we are interested in are the limit cycle's extrema

$$\begin{aligned} \gamma_{\text{min}} &= \min_{t \in [0, T_{\text{ang}}(\mathbf{p}))} \gamma(t), \\ \gamma_{\text{max}} &= \max_{t \in [0, T_{\text{ang}}(\mathbf{p}))} \gamma(t), \end{aligned} \tag{13}$$

where $\gamma(t)$ is a projection of the system's limit cycle onto the output dimension. Based on these extrema, the waveform is centered and scaled such that its amplitude extrema correspond to -1 and 1.

As with the angular period T_{ang}, these extrema are generally not available in closed form and must be estimated numerically, which will be discussed later in Section 3.2.1.

3.1.3. Equation for Tunable and Stable Signal Synthesis

By devising normalization terms based on (13), using the generalized angular frequency (12), and using the projected limit cycle γ as the source of the waveform, we arrive at the following expression for generating tunable, frequency- and amplitude-stable audio signals from nonlinear oscillators for arbitrary parameters $\mathbf{p}$:

$$\gamma_{\text{tuned}}(t) = \underbrace{\frac{1}{\gamma_{\text{min}} - \gamma_{\text{max}}}}_{\substack{\text{amplitude} \\ \text{normalization}}} \underbrace{\big(\gamma_{\text{max}} + \gamma_{\text{min}}}_{\text{waveform centering}} \underbrace{- 2\,\gamma(\hat{\omega}t)\big)}_{\text{oscillator}}. \tag{14}$$

For systems whose limit cycle is point-symmetric and centered at the origin, such as Liénard systems satisfying Liénard's original symmetry conditions, as introduced in Section 2.1, $\gamma_{\text{min}} = -\gamma_{\text{max}}$. In such cases, (14) simplifies to

$$\gamma_{\text{tuned}}(t) = \frac{\gamma(\hat{\omega}t)}{\gamma_{\text{max}}}. \tag{15}$$

3.2. Implementation Considerations

Equations (14) and (15) are idealized in the sense that they presume the availability of the limit cycle, its angular period T_{ang}, and the extrema γ_{min}, and γ_{max}. While these quantities are not analytically available for most nonlinear systems, they can be approximated in various ways. The limit cycle itself can be approximated by numerically integrating the system's differential equations. To reduce convergence time and avoid transients, initial conditions $(x(0), y(0))$ should be chosen close to the known limit cycle.

3.2.1. Offline Step Counting

For certain well-studied systems, including the van der Pol oscillator and the Brusselator, analytical approximations for period [20, 21, 22] and amplitude [14] exist. However, these approximations are often insufficiently accurate. Instead, an offline approximation step can be applied, in which the system is numerically simulated for a grid of parameter vectors $\mathbf{p}$. For each configuration, the number of steps required to complete one full period is counted. Dividing this step count by the numerical step size yields an estimate of the angular period $T_{\text{ang}}(\mathbf{p})$. Similarly, γ_{min} and γ_{max} can be tracked simultaneously. These values are then stored in a lookup table and later used when synthesizing the waveform. The use of lookup tables represents a practical tradeoff: While not the most elegant solution in a theoretical sense, they enable a general approach that can be easily adapted to a wide range of systems.

An obvious drawback of this method is that it does not scale well with the number of parameters, as each new parameter introduces an additional dimension to the lookup space. This can be somewhat mitigated by sampling parameters that the limit cycle's geometry is less sensitive to at a lower resolution.

An interesting empirical observation emerged while constructing the lookup tables for the angular period: using the same numerical method for both step-counting and real-time synthesis led to the lowest tuning error, even though the use of highly accurate solvers and root-finding algorithms would be preferable in principle. It is not entirely clear why this phenomenon occurs but it is suspected that some inaccuracies inherent to the chosen numerical method might partially cancel out when used consistently in both the step counting and synthesis stages.

Unlike the approximation of T_{ang} by step counting, determining γ_{min} and γ_{max} benefits from the use of more accurate methods. If an extremum lies between discrete samples, coarse sampling may underestimate the maximum amplitude and result in audible clipping. Alternatively, substepping around extrema or using a "fudge factor" in the synthesizer can also mitigate this.

3.2.2. Sampling

To realize the generalized angular frequency (12) in the solver, the time step size h must be adapted to the desired tuning frequency f, sampling rate f_{s}, and angular period T_{ang}. Moreover, in highly nonlinear regimes, solvers may become numerically unstable, especially for high f. This can be addressed by reducing the time step by a substepping factor S and running the solver S times per sample, giving

$$h = \frac{f T_{\text{ang}}(\mathbf{p})}{S f_{\text{s}}}. \tag{16}$$

Additionally, the higher the nonlinearity, the more likely it is that audible aliasing occurs. Oversampling arises naturally from the substepping process: the intermediate states computed during substepping can be collected, lowpass-filtered, and downsampled to obtain an antialiased audio signal. However, both the required substepping rate for numerical stability and the oversampling factor for effective antialiasing are difficult to predict in advance and are best determined empirically

4. EVALUATION AND EXPERIMENTS

This section evaluates the method proposed in Section 3 by assessing tuning accuracy and amplitude normalization for both the van der Pol oscillator and the Brusselator. It also demonstrates the tuning stability of the van der Pol oscillator under parameter modulation. Finally, two examples are presented illustrating the van der Pol oscillator and the Brusselator in sound design contexts. For all oscillators, the projection $(x(t), y(t)) \mapsto x(t)$ was chosen.

4.1. Setup

4.1.1. Lookup Table Generation

Since there are no direct or rigorous ways to determine optimal parameters for the lookup table generation, the parameters were determined empirically to minimize tuning and amplitude normalization error while keeping the offline preprocessing computationally manageable. The system parameter ranges were chosen based on numerical stability characteristics.

For the van der Pol oscillators, both the original and the modified one with a circular limit cycle at $\mu = 0$, the angular period lookup table was sampled over the parameter interval $\mu \in [0, 10]$ with a spacing of 0.1, leading to a table size of 101. The sampling was performed with an integration frequency of $1000\,\text{Hz}$. For each sample, the system was reset to initial condition $(2, 0)$ and was given one full period of "warmup time" to ensure that numerical transients could decay and that the system could settle in an equilibrium.

The Brusselator's angular period and amplitude lookup tables were sampled over the intervals $A \in [1.35, 2.2]$ and $B \in [6, 8]$ with a spacing of 0.01 for A and 0.02 for B, resulting in a size of 8686 entries per table. The integration frequency was chosen at $2000\,\text{Hz}$. Initial conditions were chosen as $(2.49, 2)$, which was found by visual inspection of several limit cycle phase portraits to be a point in the phase plane that is close to all limit cycles of the parameter sets of interest. Two periods were chosen as "warmup time" for most parameter sets. For $A >= 2.1$ and $B <= 6.5$, it was found that the system converged slowly to the limit cycle, resulting in measurable tuning and amplitude errors. To avoid this, the number of warmup periods was increased to 6 for these parameter sets.

4.1.2. Oscillator Implementation

To ensure stable, accurate, and efficient audio synthesis, several implementation decisions were made. The numerical method used for both lookup table generation and real-time synthesis was a second-order explicit Runge–Kutta integrator. While computationally inexpensive, this method suffers from accuracy and stability limitations when applied to stiff equations. Consequently, the van der Pol oscillator was restricted to a maximum frequency of $2500\,\text{Hz}$ and a maximum μ of 10, while the Brusselator was limited to $1000\,\text{Hz}$ with $A \in [1.35, 2.2]$ and $B \in [6, 8]$. Tests using a fourth-order Runge–Kutta and a three-stage Rosenbrock–Wanner solver showed no significant improvements for the Brusselator.

The oscillators were implemented with a substepping factor of 24 for numerical stability. Increasing the substepping factor further appeared to yield diminishing returns. Initially, parameter values were linearly interpolated between substeps, but this approach introduced tuning and amplitude inaccuracies. Better results were obtained by holding parameters constant across all substeps contributing to a single output sample.

To suppress aliasing, oversampling by a factor of 12 was employed in conjunction with an eighth-order Butterworth lowpass filter. Given the substepping factor of 24, every second numerically computed sample produced during substepping was collected into a buffer, filtered, and then downsampled to generate the final audio signal.

Finally, interpolation for values between lookup table entries was performed using linear interpolation for the one-dimensional parameter spaces of the van der Pol oscillators and bilinear interpolation for the two-dimensional tables of the Brusselator.

4.2. Tuning Accuracy

The oscillators were tested for tuning accuracy by sweeping their parameter spaces at differnt frequencies and recording the maximum absolute and relative deviation from the tuning frequency.

For the van der Pol oscillators, the largest relative error was found at a tuning frequency of $1790\,\text{Hz}$ with $\mu = 10$, where the measured frequency was $1805.92\,\text{Hz}$, corresponding to an error of approximately 0.889%. A higher absolute error of $21.6\,\text{Hz}$, or approximately 0.863% relative error, was found at a tuning frequency of $2500\,\text{Hz}$ with $\mu = 8.3$. By comparison, the analytical approximation to to the van der Pol oscillator's period published in [21] is slightly more accurate at high μ, giving a measured frequency of $1803.55\,\text{Hz}$ for a tuning frequency of $1790\,\text{Hz}$, corresponding to a relative error of approximately $0.757\ \%$. For lower μ, however, this approximation becomes progressively inaccurate. For example, for $\mu = 5$ and a tuning frequency of $2000\,\text{Hz}$, the measured frequency was $2026.8\,\text{Hz}$, giving a relative error of $1.34\ \%$. Using the numerically determined lookup table for the period, a frequency of $2004.2\,\text{Hz}$ was measured, amounting to $0.21\ \%$ relative error.

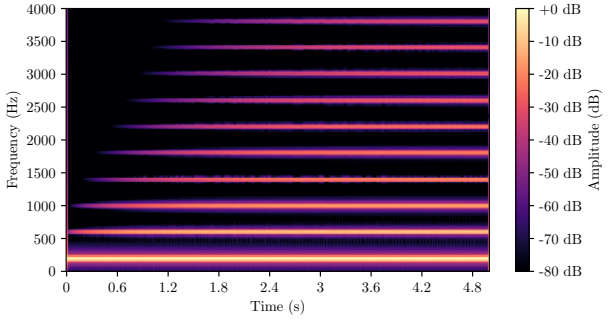

Figure 6: Spectrogram of the van der Pol oscillator with $f = 200\,\mathrm{Hz}$ and μ changing from 0 to 8.

The Brusselator, despite having a limit cycle that undergoes more pronounced deformations under parameter modulation, has better tuning accuracy than the van der Pol oscillators. Overall, its measured frequency is within $\pm 2\,\mathrm{Hz}$ of the tuning frequency for most parameter choices and tuning frequencies. The most extreme tuning errors were found with parameter B at its maximum of 8. With $A = 2.2$, the maximum absolute tuning error was found at a tuning frequency of $1000\,\mathrm{Hz}$ with a measurement of $997.2\,\mathrm{Hz}$ and $0.28\ \%$ relative error. Tuning error increased as A was reduced with a maximum detuning of $-4.5\,\mathrm{Hz}$ at $A = 1.35$, corresponding to a relative error of 0.45%.

4.3. Tuning Stability

Tuning stability was evaluated by synthesizing a continuous five-second tone using a van der Pol oscillator tuned to $200\,\mathrm{Hz}$. Over this duration, its tuning was not changed, while the damping parameter μ was linearly swept from 0 to 8. Figure 6 depicts the resulting spectrogram and shows no significant pitch instability.

4.4. Amplitude Normalization Accuracy

The accuracy of amplitude normalization was investigated by synthesizing waveforms of the implemented oscillators and measuring the difference between the highest peaks and unity.

For the van der Pol oscillators, no sophisticated amplitude normalization was implemented since their limit cycles are point-symmetric and their maximum of x is close to 2 for all μ. Consequently, it was assumed that using a gain normalization factor 0.5 would be sufficient to avoid clipping. However, it was measured that the largest magnitude of 1.209 occurs at at $\mu = 10$ and a tuning frequency of $2500\,\mathrm{Hz}$. The addition of a correction factor of 0.828 counteracted the clipping issue but also reduced the magnitude, to approximately the same quantity as the correction factor for low frequencies and low values of μ.

Despite already adjusting the amplitude using the values measured in the offline processing step, the Brusselator too exhibited undesirably high magnitudes. The magnitude observed was $1,205$ for $A = 1.35$, $B = 8$, in the frequency range of $170\,\mathrm{Hz}$ to $200\,\mathrm{Hz}$. As with the van der Pol oscillators, the addition of an additional correction factor prevented clipping but reduced the signal magnitude to significantly below unity for other frequencies and parameter choices.

In both oscillators, these issues arise in settings where the systems are highly stiff and evolve rapidly, leading to two main problems. First, as mentioned in Section 3.2.1, when the system's dynamics evolve quickly, the limit cycle's actual extrema may fall in-between two sample points, leading to an underestimation of the waveform's magnitude, and therefore insufficient gain reduction. Second, in stiff regimes, especially at high frequencies, the solvers operate at the limits of their numerical stability. In such nearly-unstable scenarios, high-frequency, often inaudible, noise is introduced by numerical artifacts and pollute the synthesized audio signal. While more sophisticated and computationally expenive solvers would mitigate these effects, they can also be addressed by using a frequency- and parameter-dependent correction function in place of a constant correction factor, or by simply limiting the maximum oscillator frequency further.

4.5. Van der Pol Frequency Modulation

Frequency modulation (FM) synthesis is traditionally performed using sinusoidal oscillators [23] due to their harmonic simplicity. However, the van der Pol oscillator approximates a simple harmonic oscillator at low values of μ, especially in the modified variant introduced in Section 2.2, which retains a circular limit cycle even at $\mu = 0$. This makes it a promising candidate for FM synthesis, with the added benefit of enriching the spectrum controllably through the parameter μ.

An FM synthesizer was constructed with two carriers, each driven by a separate modulator, all of which were sinusoidal. Parameter values were chosen to produce bell-like tones. In the first experiment, the carriers were replaced with van der Pol oscillators whose μ values were modulated by a decaying envelope, starting at $\mu = 2$ and decreasing to zero within $200\,\mathrm{ms}$. The excitation envelope was also shortened, and the base frequency slightly lowered. The resulting sounds had more energy in the transients, making them percussive and metallic. These transients emerged naturally from the nonlinear response of the oscillator depending on μ.

In a second experiment, the modulators were also replaced by van der Pol oscillators with $\mu = 9$. This configuration produced distorted, "thumpy" metal impact sounds with a rougher spectral texture, showcasing the oscillator's potential for nonlinear modulation effects beyond purely sinusoidally-based FM synthesis.

4.6. Brusselator Supersaw

The Supersaw waveform, famously introduced by Roland's JP-8000 and JP-8080 synthesizers, consists of several detuned sawtooth oscillators playing at once. The Brusselator's limit cycle also exhibits a waveform resembling a sawtooth, as discussed in 2.3.1, suggesting its potential use in a Supersaw-style configuration.

To evaluate this potential, a synthesis setup modeled after Szabo's analysis of the original Supersaw [24] was implemented, consisting of seven detuned sawtooth oscillators. A second version of the patch replaced the sawtooth oscillators with Brusselators.

At parameter settings near $A = 2.2$, $B = 8$, which are the upper bounds supported by the implementation, the resulting sound closely matched that of the traditional Supersaw. As B was reduced from 8 to 6, the overall timbre became softer, similar to the effect of a gradually lowering low-pass filter.

5. CONCLUSION

This work investigated the synthesis of audio signals from nonlinear dynamical systems exhibiting stable limit cycles. Two representative systems, the van der Pol oscillator and the Brusselator, were studied as case examples. A method was proposed that enables tuning the oscillator frequency and amplitude and keeping them stable independently of changes to the underlying system's parameters. This approach was derived from the geometry of the limit cycle and discussed with respect to its practical implementation, including normalization, lookup table generation, and oversampling. The method's accuracy and its limitations were assessed quantitatively and qualitatively by example.

Synthesis examples demonstrated that tunable nonlinear oscillators lend themselves well to creative sound design. In an FM synthesis context, the van der Pol oscillator served as a rich transient generator for percussive and impact-like sounds. The Brusselator, whose waveform resembles a sawtooth for certain parameter ranges, was used in a Supersaw-style oscillator bank. For specific configurations, it was found to be similar to a standard sawtooth-based Supersaw, whereas certain choices of parameter values exhibited lowpass characteristics.

5.1. Future Work

Several directions remain open for future exploration. One particularly interesting area is the use of multistable systems with more than one stable limit cycle. The method presented here is already applicable to such systems, provided that each stable limit cycle is treated as a distinct oscillator with its own lookup tables and numerical solver. Synthesizing audio signals from multiple limit cycles simultaneously enables many creative possiblities, such as tuning each attractor to a different frequency to form chords, or to the same frequency to produce layered unison textures. However, when generating the lookup tables for a multistable system, the initial conditions must be chosen carefully to ensure convergence to the intended attractor, especially when the basins of attraction are narrow. Furthermore, if an oscillator in a multistable system is perturbed from its trajectory, for example by a driving force, it can switch trajectories and settle into a different limit cycle. Such switching behavior should either be avoided or detected in real time so that the appropriate limit cycle's lookup tables can be applied dynamically.

An additional direction for future work lies in studying the chaotic behavior that arises from nonautonomous modifications of nonlinear oscillators, such as the addition of driving forces, delayed feedback, audio-rate parameter modulation, and oscillator coupling. While modifications of this kind are well known in dynamical systems theory and have been explored in audio processing and sound design, it remains to be studied whether tunable oscillators exhibit novel behaviors under such conditions.

Finally, another direction for future research is to overcome the stability constraints of numerical integration methods, which currently limit the applicability of the presented approach. Nonlinear oscillators often exhibit significant stiffness over part of their parameter space, leading to constraints on the usable frequency and parameter range. A deeper investigation into numerical methods optimized for real-time synthesis of stiff nonlinear systems may help extend the practical applicability of these techniques. If such methods reduce the need for substepping, this may also open the door to using bandlimited ramp (BLAMP) techniques as an alternative or improvement to oversampling for antialiasing. This could be especially beneficial for oscillators with near-discontinuities, such as the Brusselator.

5.2. Supplementary Materials

The implementation, audio examples, and supplementary materials, including Pure Data objects, example patches, and Python scripts used in evaluation, are available at `https://wolframw.github.io/stable-limit-cycles/`.

6. REFERENCES

[1] Georg Essl, "Exploring the Sound of Chaotic Oscillators via Parameter Spaces," in *Proceedings of the 22nd International Conference on Digital Audio Effects (DAFx-19)*, Sept. 2019.

[2] Miller Puckette, "A Quaternion-Phase Oscillator," in *Proceedings of the 25th International Conference on Digital Audio Effects (DAFx20in22)*, Sept. 2022.

[3] Nick Collins, "Errant Sound Synthesis," in *International Computer Music Conference*, Aug. 2008.

[4] Perry R. Cook, *Real Sound Synthesis for Interactive Applications*, A K Peters, 2002.

[5] Gijs de Bruin and Maarten van Walstijn, "Physical Models of Wind Instruments: A Generalized Excitation Coupled with a Modular Tube Simulation Platform," *Journal of New Music Research*, vol. 24, no. 2, pp. 148–163, 1995.

[6] Xavier Rodet, "Nonlinear Oscillator Models of Musical Instrument Excitation," in *ICMC: International Computer Music Conference*, Oct. 1992, pp. 412–413.

[7] Dario Sanfilippo, "modified_van_der_pol," GitHub, Mar. 2021, `https://github.com/dariosanfilippo/modified_van_der_pol`.

[8] Oswald Berthold, "nloscs," GitHub, Apr. 2017, `https://github.com/x75/nloscs`.

[9] Risto Holopainen, "Nonlinear Oscillators and Frequency Modulation," 2020, `https://ristoid.net/modular/nonlin_osc.html`.

[10] Steven H. Strogatz, *Nonlinear Dynamics and Chaos With Applications to Physics, Biology, Chemistry, and Engineering*, CRC Press, third edition, 2024.

[11] Gabriele Villari and Fabio Zanolin, "On the uniqueness of the limit cycle for the Liénard equation with $f(x)$ not sign-definite," *Applied Mathematics Letters*, vol. 76, pp. 208–214, 2018.

[12] Makoto Hayashi, Gabriele Villari, and Fabio Zanolin, "On the uniqueness of limit cycle for certain Liénard systems without symmetry," *Electronic Journal of Qualitative Theory of Differential Equations*, vol. 2018, pp. 1–10, June 2018.

[13] Balthasar van der Pol, "A Theory of the Amplitude of Free and Forced Triode Vibrations," *The Radio Review*, vol. 1, no. 14, pp. 701–710, Nov. 1920.

[14] Jose L. López, Saeid Abbasbandy, and Ricardo López-Ruiz, "Formulas for the Amplitude of the van der Pol Limit Cycle through the Homotopy Analysis Method," *Scholarly Research Exchange*, vol. 2009, no. 1, Apr. 2009.

[15] Venus Pasandi, Aiko Dinale, Mehdi Keshmiri, and Daniele Pucci, "A Data Driven Vector Field Oscillator with Arbitrary Limit Cycle Shape," in *2019 IEEE 58th Conference on Decision and Control (CDC)*. Dec. 2019, pp. 8007—8012, IEEE.

[16] Garrett Birkhoff and Gian-Carlo Rota, *Ordinary Differential Equations*, John Wiley & Sons, 4th edition, 1991.

[17] Ferdinand Verhulst, *Nonlinear Differential Equations and Dynamical Systems*, Springer, second edition, 2000.

[18] Evgeni Sel'kov, "Self-Oscillations in Glycolysis," *European Journal of Biochemistry*, vol. 4, no. 1, pp. 79–86, Mar. 1968.

[19] Ilya Prigogine and René Lefever, "Symmetry Breaking Instabilities in Dissipative Systems. II," *The Journal of Chemical Physics*, vol. 48, no. 4, pp. 1695–1700, Feb. 1968.

[20] Shaun Ault and Erik Holmgreen, "Dynamics of the Brusselator," Mar. 2003, `https://mate.unipv.it/boffi/teaching/download/Brusselator.pdf`.

[21] Anatoly A. Dorodnicyn, "Asymptotic Solution of Van Der Pol's Equation," Apr. 1953.

[22] Carl M. Andersen and James F. Geer, "Power Series Expansions for the Frequency and Period of the Limit Cycle of the Van Der Pol Equation," *SIAM Journal on Applied Mathematics*, vol. 42, no. 3, pp. 678–693, 1982.

[23] John M. Chowning, "The Synthesis of Complex Audio Spectra by Means of Frequency Modulation," *Computer Music Journal*, vol. 1, no. 2, pp. 46–54, Apr. 1977.

[24] Adam Szabo, "How to Emulate the Super Saw," 2010, `https://www.adamszabo.com/internet/adam_szabo_how_to_emulate_the_super_saw.pdf`.